Coassembly of Block Copolymer and Randomly Methylated β-Cyclodextrin: From Swollen Micelles to Mesoporous Alumina with Tunable Pore Size

ARTICLE *in* MACROMOLECULES · JULY 2013

Impact Factor: 5.8 · DOI: 10.1021/ma4008303

5 AUTHORS, INCLUDING:

Rudina Bleta
Université d'Artois
16 PUBLICATIONS **180** CITATIONS
SEE PROFILE

Cécile Binkowski Machut
Université d'Artois
22 PUBLICATIONS **193** CITATIONS
SEE PROFILE

Bastien Leger
University of Lille Nord de France
32 PUBLICATIONS **482** CITATIONS
SEE PROFILE

Eric Monflier
Université d'Artois
238 PUBLICATIONS **3,795** CITATIONS
SEE PROFILE

Macromolecules

Article

pubs.acs.org/Macromolecules

Coassembly of Block Copolymer and Randomly Methylated β-Cyclodextrin: From Swollen Micelles to Mesoporous Alumina with Tunable Pore Size

Rudina Bleta,[†,‡,§] Cécile Machut,[†,‡,§] Bastien Léger,[†,‡,§] Éric Monflier,[†,‡,§] and Anne Ponchel*[,†,‡,§]

[†]Université Lille Nord de France, F-59000 Lille, France

[‡]UCCS, Faculté des Sciences Jean Perrin, Université d'Artois, Rue Jean Souvraz, SP 18, F-62307 Lens, France

[§]CNRS, UMR 8181, F-59650 Villeneuve d'Ascq, France

ABSTRACT: Controlling interactions at the supramolecular level is of importance for the preparation by template directed synthesis of mesoporous materials with tailored pore structures. Herein we investigate the effect of randomly methylated β-cyclodextrin on the association behavior of the amphiphilic triblock copolymer Pluronic P123 in aqueous solution. Surface tension, dynamic light scattering, and viscosity measurements provide quantitative evidence that, when the cyclodextrin is added in controlled amounts to the copolymer, it strongly impacts the micellar growth rate. The property of randomly methylated β-cyclodextrin to act as a micelle expander has been further exploited to generate a series of mesoporous γ-alumina by a sol−gel method. The resulting materials subjected to calcination at 500 °C exhibit high surface area (354−382 m^2/g), tunable pore size (14.8−19.3 nm), and very large pore volume (1.37−1.97 cm^3/g), making them excellent candidates for applications in the fields of adsorption and heterogeneous catalysis.

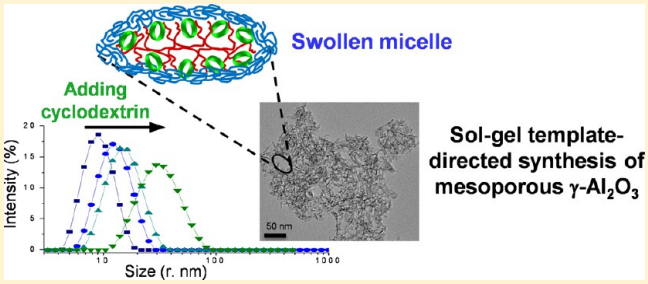

INTRODUCTION

In recent years, a great deal of attention has been focused on the design and construction of nanoscale ordered structures by supramolecular self-assembly. In particular, well-defined macromolecular architectures with a variety of intriguing structures have been obtained from host−guest interactions between amphiphilic surfactants and cyclodextrins.[1−6] Such supramolecular structures constitute a very active topic of research with a number of potential applications in the field of nanoscience as molecular nanotubes,[7] molecular wires,[8] and smart materials with stimuli responsiveness.[9] Under appropriate solution conditions, amphiphilic surfactants, such as for instance block copolymers, can self-assemble into micelles to form a hydrophobic core and a hydrated corona with spherical, cylindrical, or ellipsoidal shapes.[10] Cyclodextrins (CDs) are water-soluble cyclic oligosaccharides formed of *n* glucopyranose units exhibiting a hydrophobic internal cavity and a hydrophilic exterior surface due to the presence of a large number of hydroxyl groups. These molecules demonstrate multifunctional properties, such as the formation of supramolecular adducts or host−guest inclusion complexes with a large number of molecules of appropriate size and shape.[11,12] The most common cyclodextrins are α-, β-, and γ-cyclodextrins having 6, 7, and 8 glucose units in the ring, respectively, and among them, β-CD has received the greatest attention, due to its high overall binding affinity and cost effectiveness.

Since the pioneering works of Harada et al.,[13,14] who showed that α-CD can form inclusion complexes with poly(ethylene glycol) (PEG) in aqueous solution to give polypseudorotaxanes with a necklace-like structure, a range of polymeric guests have been found to form inclusion complexes with cyclodextrins.[15] A particular attention has been paid to the interactions occurring between the native β-CD and nonionic triblock copolymers of the poly(ethylene oxide) (PEO)-*b*-poly(propylene oxide) (PPO)-*b*-poly(ethylene oxide) (PEO) family, also known as Pluronics.[16−19] Thus, it has been shown that the native β-CD can slide along the hydrophilic extremity PEO blocks of the Pluronic P84 ($PEO_{19}PPO_{43}PEO_{19}$) to selectively thread the middle hydrophobic PPO blocks forming polypseudorotaxanes, as evidenced by ^{1}H NMR and circular dichroism.[16,17] The possibility of using cyclodextrins as additives in the design of micellar-ordered structures has also been the subject of several investigations.[20,21] Recent studies have revealed that supramolecular assemblies with a very rich structural polymorphism can be generated from specific host−guest interactions.[18,19] Thus, Tsai et al.[18] have shown that inclusion complexes with a well-ordered channel configuration resulting from the interactions between β-CD and PPO blocks could be formed below the critical micellization concentration (CMC). Remarkably,

Received: April 23, 2013
Revised: June 23, 2013
Published: July 5, 2013

   dx.doi.org/10.1021/ma4008303 | *Macromolecules* 2013, 46, 5672−5683

these channel-like inclusion complexes were shown to spontaneously self-assemble in water to generate supramolecular assemblies with a well-defined crystalline structure. By using small-angle neutron scattering and atomic force microscopy, Schlatter et al.[19] have provided experimental evidence of the fact that the self-assembly of β-CD and Pluronic F68 copolymer micelles ($PEO_{80}PPO_{27}PEO_{80}$) leads to the formation of cylindrical bundles, which can further act under appropriate conditions as building blocks to form flat and rigid platelets with well-defined angles. In addition, the authors have also reported that the self-assembly of Pluronic F68 and native β-CD is sensitive to temperature changes. Whereas stable β-CD-swollen micelles were observed at a high temperature, i.e. 70 °C, a disruption of the micelles occurred when the mixture was thermally quenched at temperatures below the critical micellization temperature, i.e. 40 °C, due to the inclusion complex formation.

Compared to the native β-CD, the interactions between modified β-CDs and block copolymers have been less investigated in the literature, and the few studies available on this subject have given rise to divergent interpretations. Thus, the results reported by Gaitano et al.,[22] and later supported by other authors,[23−27] have shown that, similarly to native β-CD, the macrocycle of a dimethylated β-CD is able to form polypseudorotaxanes with the hydrophobic PPO blocks of different Pluronic copolymers. Conversely, in a more recent study, spectroscopic and time-resolved small-angle neutron scattering measurements conducted on mixtures of heptakis-(2,6-di-*o*-methyl)-β-CD and Pluronics, such as F127 ($PEO_{107}PPO_{70}PEO_{107}$), P85 ($PEO_{39}PPO_{52}PEO_{39}$), and P123 ($PEO_{20}PPO_{70}PEO_{20}$), evidenced that the micellar rupture occurs with extremely fast kinetics, excluding the possibility of forming polypseudorotaxanes via inclusion complexes.[28] Interestingly in the case of Pluronic P123, the authors have reported a possible restructuration of the micelles toward swollen lamella, with an interlayer spacing much higher than the typical values reported in literature with conventional swelling agents.[29] However, the phenomenon of micellar rupture cannot be generalized to all cases. Indeed, the nature of the interactions involved in the self-assembly was shown to be highly sensitive to substitution degree, nature, and position of the modified cyclodextrins.[23,28] Thus, in contrast to the micellar rupture observed with the heptakis (2,6-di-*o*-methyl)-β-CD, Dreiss et al.[28] have shown that, under similar experimental conditions, the micelles remained intact in the presence of other substituted β-cyclodextrin derivatives, such as the 2,3,6-trimethyl-β-CD, 2-hydroxyethyl-β-CD, and 2-hydroxypropyl-β-CD.

Despite their rich structural polymorphism, the supramolecular assemblies formed between block copolymers and cyclodextrin derivatives have been little used as soft templates for the synthesis of hierarchically structured porous materials. In the field of nanocasting, only a few studies have reported the possibility of using cyclodextrins or cyclodextrin/polymer mixtures as supramolecular templates, and most of them have been devoted to the synthesis of mesoporous silica by the sol−gel process.[30−32] The synthesis procedure, which combines a templating approach with sol−gel chemistry, is known to be one of the most important strategies in modern material science, owing to its ability to tailor the pore size by manipulating the size of the templating micelles.[33−35] However, this method requires a careful control of the structural characteristics of the micelles, in terms of size or morphology.[35] Interestingly, the possibility of using block copolymer assemblies as templates, in combination or not with swelling agents (e.g., alkyl-substituted benzenes), was successfully reported to give hierarchical structures with significantly enlarged pores.[36,37]

In the present study, we have investigated the supramolecular associations occurring between the Pluronic P123 block copolymer and randomly methylated β-cyclodextrin, with the attempt to use these assemblies as novel candidates for the template-assisted synthesis of porous inorganic solids. Surprisingly and to our knowledge, the interactions between the randomly methylated β-cyclodextrin and block copolymers have not yet been reported in the literature. The randomly methylated β-CD (denoted as RAMEB where methylation occurs at the C2, C3, or C6 positions with statistically 1.8 OH groups modified per glucopyranose unit) can be seen as a versatile structure directing agent. Indeed, this cyclodextrin is highly soluble in water, cheap, nontoxic, and commercially available[38] and has the property of being surface active.[39,40] When used in association with polymers, it can be considered that RAMEB gives rise to well-defined water-soluble supramolecular structures, which can act as templates for the self-assembly of nanoparticles in a homogeneous mesophase. For that purpose, in a first part, we have undertaken a detailed investigation of the impact of RAMEB on the micellization process by means of several techniques, including surface tension, dynamic light scattering, and viscosity measurements. Different ratios of RAMEB to Pluronic P123 have been employed to obtain insight into the role of this β-cyclodextrin in the nanoparticle self-assembly process. In a second part, our motivation was to take advantage of the physicochemical properties of RAMEB and their ability to interact with Pluronic P123 to elaborate a series of mesoporous alumina with adjustable pore size and pore volume by applying the nanoparticle route.[34,41] From the viewpoint of synthesis, it is still a challenge to synthesize mesoporous alumina with adjustable porosity[41,42] while the applications of this material are known to be of practical importance in different areas of material science, due to its high mechanical strength as well as high chemical and thermal stability.[43−45] The ability of RAMEB to promote the formation of mesoporous alumina with tailored porosity is discussed on the basis of N_2 adsorption−desorption isotherms, transmission electron microscopy, infrared spectroscopy, and X-ray diffraction measurements.

EXPERIMENTAL SECTION

Chemicals. The PEO−PPO−PEO triblock copolymer [PEO = poly(ethylene oxide) and PPO = poly(propylene oxide)], denoted Pluronic P123, was purchased from Sigma-Aldrich. It has an average composition of $PEO_{20}PPO_{70}PEO_{20}$ and a molar weight (M_w) of 5800 g/mol. Randomly methylated β-cyclodextrin (denoted RAMEB with an average degree of molar substitution of 1.8 (M_w 1310 g/mol)) was a gift from Wacker Chemie GmbH. Aluminum tri-*sec*-butoxide, $Al(OCC_3H_9)_3$ (referred to as ASB, M_w 246.32 g/mol), and nitric acid (HNO_3, 68 wt %) were procured from Sigma-Aldrich. All chemicals were used as received without further purification.

Preparation of the RAMEB/P123 Mixtures for the Characterization. 100 mL of a 7.8 wt % Pluronic P123 micellar solution was produced by dissolving the appropriate amount of copolymer (7.8 g) in double distilled water (100 mL) under stirring at room temperature. Subsequently, aliquots of 10 mL micellar solution were placed into glass cells and various amounts of RAMEB were added, in the concentration range of 5−130 mg/mL (corresponding to RAMEB/P123 molar ratios of 0.3−7.1). The mixtures were stirred for 30 min

dx.doi.org/10.1021/ma4008303 | Macromolecules 2013, 46, 5672−5683

then allowed to equilibrate in a thermostatic bath at 25 °C for 24 h before analysis.

Synthesis of Mesoporous Alumina. Boehmite (AlO(OH)) nanoparticles were used as inorganic precursor for the preparation of mesoporous alumina. Nanoparticles were synthesized by a sol−gel method reported by Yoldas.[46] In a dry 250 mL flask, 185 mL of hot distilled water (85 °C) was added fast to 25.3 g (0.1 mol) of ASB at a hydrolysis ratio of 100 (h = H_2O/Al). After 15 min, the hydroxide precipitate was peptized by adding dropwise 0.474 mL (0.1 mol) of HNO_3 ([HNO_3]/[Al] = 0.07). The white precipitate was stirred at 85 °C for 24 h. The final product was a transparent suspension of boehmite nanoparticles (pH 4.4−4.8). Under these conditions, the concentration of aluminum in the sol was determined by weight loss on ignition at 1000 °C and was estimated to be 0.55 mol/L.[47] Subsequently, Pluronic P123 (7.8 wt %, PEO/Al = 1) was added in the nanoparticle sol, and the mixture was stirred for 3 h at room temperature. 10 mL aliquots of copolymer/boehmite sols were transferred into glass vials, and various amounts of RAMEB (30−130 mg/mL, RAMEB/P123 molar ratio = 1.7−7.1) were added. The sols were stirred for an additional 30 min and then allowed to equilibrate at room temperature for 24 h. Xerogels were recovered after drying 10 mL samples by evaporation at 60 °C for 48 h, after which time they were calcined in air at 500 °C for 16 h using a heating ramp of 1 °C/min. Mesoporous γ-Al_2O_3 were identified according to the following notation: Px-CDy-Al-Tz, where x is the PEO/Al molar ratio, y is the RAMEB concentration (mg/mL), and z is the calcination temperature (°C). For example, Al-T500 indicates a mesoporous alumina calcined at 500 °C prepared without copolymer and without cyclodextrin (control), whereas P1-CD30-Al-T500 indicates a mesoporous alumina prepared with a PEO/Al molar ratio of 1, a RAMEB concentration of 30 mg/mL in the sol (i.e., CD/P123 = 1.7), and a calcination temperature of 500 °C.

Characterization Methods. *Surface Tension Measurements.* Surface tension of pure aqueous solutions of RAMEB, Pluronic P123, and mixtures of RAMEB/Pluronic (CD/P123 molar ratio = 1.7−7.1) were determined by successive dilutions using an automatic Sigma 701 tensiometer (Attension, KSV Instruments Ltd.). Measurements were performed at 25 °C with the Wilhelmy plate technique. Average values of surface tension were obtained from three consecutive measurements. Before each series of measurements, samples were carefully filtered through a Millipore filter with a 0.2 μm pore size to remove any impurities. The surface tension of double distilled was measured before each series of measurements until a value of 72 mN/m was reached.

Dynamic Light Scattering (DLS). DLS measurements were performed at 25 °C by using a Malvern Zeta Nanosizer instrument. The apparatus is equipped with a 4 mW He−Ne laser operating at 633 nm and uses a backscattering detection system (scattering angle θ = 173°). Samples were filtered through a 0.2 μm Millipore filter before analysis. The quantity measured in DLS is the time correlation function (TCF) of the scattered intensity $g^{(2)}(t)$[48] which was obtained directly from the software during the measurement. TCF is described as an exponential decay which originates from the Brownian motion of the micelles and depends on their diffusivity. TCFs were analyzed by the CONTIN method[49] to obtain distribution decay rates (Γ). The apparent diffusion coefficient (D) was then determined from Γ: $D = \Gamma/q^2$, where q is the scattering vector, $q = (4\pi n/\lambda)\sin(\theta/2)$, n is the refractive index of the solution, and λ is the incident laser wavelength.

The apparent hydrodynamic radius (R_h) was deduced from the diffusion coefficient D using the Stokes−Einstein formula: $R_h = K_B T/6\pi\eta D$, where K_B, T, and η are the Boltzmann constant, the absolute temperature, and the viscosity of water at the temperature T, respectively. Each DLS experiment was repeated in triplicate.

Viscometry. The apparent viscosities of the solutions were measured in a temperature-controlled water bath by using a viscosimeter from Brookfield equipped with a cylindrical geometry (module SC4-18). The apparent viscosity vs shear rate plots were recorded at 25 °C with a shear rate being stepwise increased over the range of 1−130 s^{-1}.

Nitrogen Adsorption−Desorption. Isotherms were collected at −196 °C using an adsorption analyzer Micromeritics Tristar 3020. Prior to analysis, samples (200−400 mg) were outgassed at 320 °C overnight to remove the species adsorbed on the surface. From N_2 adsorption isotherms, specific surface areas were determined by the BET method and pore size distribution was calculated by a software (Autosorb 1 from Quantachrome Instruments) based on the NLDFT (nonlocal density functional theory) model[50] assuming a cylindrical pore structure. Pore volume (P_v) was calculated from the adsorbed volume (V_a) at a relative pressure of 0.995.

Transmission Electron Microscopy (TEM). TEM observations were performed on a Tecnai microscope operating at an accelerating voltage of 200 kV at medium magnification. A drop of alumina powder suspension dispersed in ethanol was deposited on a carbon-coated copper grid.

Attenuated Total Reflection Fourier Transform Infrared (ATR-FTIR). FTIR-measurements were carried out on a Shimadzu IR Prestige-21 spectrometer equipped with a MIRacle Diamond prism. Spectra were recorded in the 4000−500 cm^{-1} region with a spectral resolution of 2 cm^{-1}.

Powder X-ray Diffraction (XRD). XRD data were collected on a Siemens D5000 X-ray diffractometer in a Bragg−Brentano configuration with a Cu Kα radiation source. XRD scans were run over the angular domain 10° < 2θ < 80° with a step size of 0.02° and a counting time of 2 s per step.

RESULTS

Interactions between Randomly Methylated β-Cyclodextrin and P123 Copolymer in Aqueous Solution. Figure 1 shows the visual aspect of the Pluronic P123 aqueous solutions (7.8 wt %) prepared with increasing amounts of RAMEB in the range of 0−130 mg/mL.

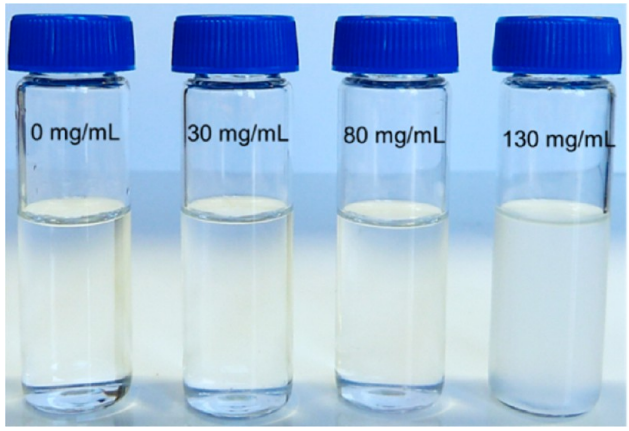

Figure 1. Visual aspect of the P123 solutions (7.8 wt %) prepared with increasing amounts of RAMEB at 25 °C (from left to right: 0, 30, 80, and 130 mg/mL).

It can be seen that the solution prepared without cyclodextrin is transparent at 25 °C, indicating that the dominating species are the Pluronic micelles, in agreement with the phase diagram of this copolymer in water.[51] With increasing the concentration of RAMEB from 30 to 80 mg/mL, the Pluronic solutions still remain homogeneous and transparent, whereas for 130 mg/mL, the mixture becomes turbid, indicating the formation of large scattering species. Note that such turbidity is not observed with pure RAMEB solutions in the investigated concentration range since this cyclodextrin is very soluble in water (>300 mg/mL). This suggests that the interactions between RAMEB and copolymer are probably at

dx.doi.org/10.1021/ma4008303 | Macromolecules 2013, 46, 5672−5683

the origin of the formation of large scattering species in our samples.

To provide further information about the RAMEB/copolymer interactions and their impact on the micellization process, surface tension measurements were then carried out. If the hydrophobic interactions between the PPO chains, which are known to be the driving force for the micellization, are screened by the presence of the cyclodextrin, this may lead to a disruption of the copolymer micelles and an increase in the CMC. The degree of shift in the CMC is indicative of the strength of the cyclodextrin/copolymer interactions; the higher the CMC shift, the stronger the copolymer/cyclodextrin interactions. Figure 2 shows the surface tension plots recorded

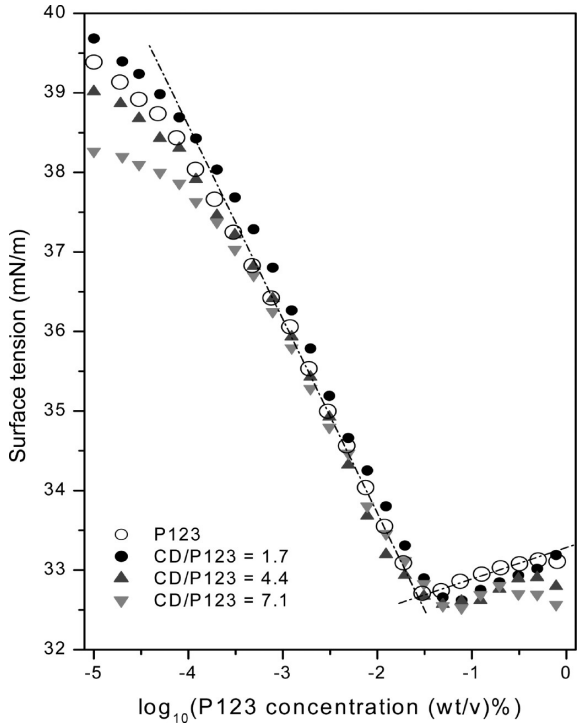

Figure 2. Surface tension plots of P123 in water without and with RAMEB (CD/P123 = 1.7−7.1) as a function of concentration at 25 °C.

at 25 °C for Pluronic P123 solutions prepared without and with RAMEB (CD/P123 molar ratios in the range of 1.7−7.1). The surface tension plot of Pluronic in water shows a well-defined break point which represents the concentration at which the micelles are formed (CMC). The CMC found for this copolymer is ∼0.03 wt % (log P123 = −1.51), in agreement with the values reported in the literature.[51,52] It is worth noting that, in the vicinity of the CMC value (ranging from ∼0.03−0.04 wt %), the surface tension of the copolymer is not significantly affected by the addition of RAMEB whatever the molar ratio of RAMEB to P123 used. The effect of RAMEB becomes visible only at high dilutions, with a surface tension that decreases slightly from 39.5 to 38.3 mN/m with increasing cyclodextrin concentration. Taken together, these results suggest that the interactions between Pluronic and RAMEB are relatively weak and do not significantly affect the micellization process. Indeed, an increase in the apparent CMC could be expected if the host−guest complexation between the cavity of the cyclodextrin and the polymer controlled the coassembly process, as previously evidenced in the literature.[53,54]

To investigate whether the cyclodextrin has an impact on the copolymer micellar growth, dynamic light scattering (DLS) measurements were also performed at 25 °C. Thus, Figure 3 shows the correlation function and size distribution plots of P123 (7.8 wt %) and RAMEB (30 mg/mL) solutions, analyzed both separately and in mixture.

As can be noticed, the correlation function of pure P123 solution is a single exponential indicating a monodisperse sample. The apparent hydrodynamic radius (R_h) of the copolymer aggregates, calculated from the decay times using the Stokes−Einstein equation, is centered at 9.1 nm, and this value is in agreement with that reported by Kadam et al. (9.4 nm at 30 °C).[55] This confirms that micelles are the main scattering species in the P123 solution according to the phase diagram of this copolymer in water.[51]

In contrast, the correlation function of RAMEB solution is more complex and can be fitted to a biexponential function indicating two types of populations. Accordingly and as previously reported in the literature,[56,57] the corresponding size distribution plot is bimodal, with a first population centered at ∼0.9 nm, corresponding to isolated cyclodextrin molecules and a second population at ∼100 nm associated with cyclodextrin aggregates. Interestingly, it can be seen that, when RAMEB and Pluronic are mixed together, the cyclodextrin aggregates formed at ∼100 nm abruptly disintegrate while the isolated cyclodextrin molecules disappear, giving rise to scattering objects with a monomodal size distribution centered at 9.1 nm, which is the same apparent R_h value as that previously obtained for the pure P123 micelles. This result is an indication that RAMEB preferentially interacts with the copolymer rather than remaining solubilized in the continuous aqueous phase probably because of its higher affinity for the micellar environment.

To have a deeper insight in the location of RAMEB within the P123 micelles, we extended the domain of investigation to a broader range of cyclodextrin concentrations (5−130 mg/mL). Figure 4 displays the DLS plots of the samples prepared by progressively increasing the cyclodextrin amount in the micellar solution from 5 to15 mg/mL (Figure 4a,b) and 30 to 130 mg/mL (Figure 4c,d).

One can note that, in the range of 5−15 mg/mL RAMEB, the correlation function is not shifted and the micellar size remains constant, with a value centered at 9.1 nm. However, sharper and better resolved peaks are obtained in the size distribution plot, suggesting the formation of a larger amount of well-defined objects. This result may be explained by the preferential location of the oligosaccharide molecules in the water-rich corona region of the P123 micelles, where they preferentially interact with the hydrophilic PEO blocks of the copolymer by hydrogen bonding through their hydroxyl groups.

In contrast, for higher RAMEB concentrations, a shift of the correlation function toward larger time scales is clearly observed, indicative of a time-dependent growth of the micelles. Thus, the corresponding size distribution plots indicate a progressive increase in the apparent micellar hydrodynamic radius from 9.1 to 15.5 nm with increasing the RAMEB concentration from 30 to 80 mg/L, respectively. Even though the DLS gives access only to apparent hydrodynamic radii, this technique provides a useful indication of the structural changes

dx.doi.org/10.1021/ma4008303 | Macromolecules 2013, 46, 5672−5683

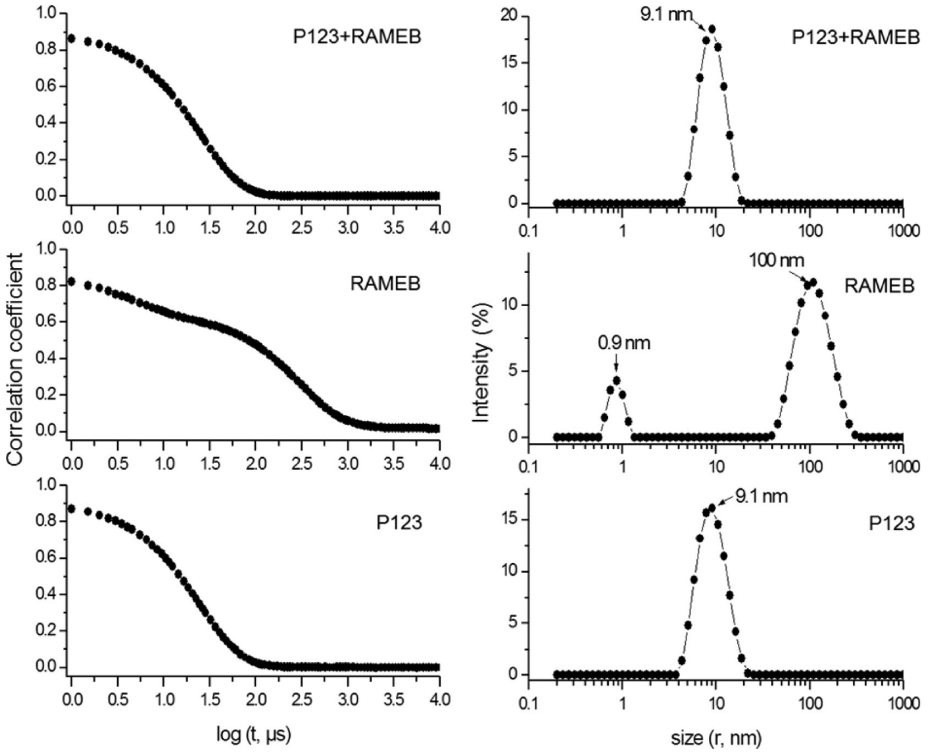

Figure 3. Correlation functions and apparent hydrodynamic radius (R_h) distributions of the scattered intensity for P123 solution (7.8 wt %), RAMEB solution (30 mg/mL), and P123/RAMEB mixtures (7.8 wt % P123 and 30 mg/mL CD) at 25 °C.

occurring within the micelles during the coassembly process between block copolymer and RAMEB.

Such variation could be attributed to the fact that methylated cyclodextrins act as swelling agents for the P123 micelles. Indeed, RAMEB with an average of about 12.6 methoxy groups per cyclodextrin tends to have more important lipophilic domains than the native β-CD, leading to a higher affinity for the hydrophobic core of block copolymer micelles. Therefore, it can be assumed that, in this concentration range, additional hydrophobic interactions occur between the OCH_3 groups of the cyclodextrin and the PPO blocks of the copolymer, resulting in the preferential location of the cyclodextrin in the PEO−PPO interface layer and stabilization of RAMEB-loaded polymeric micelles. However, when examining in more detail the DLS profiles, the scattering intensity of these assemblies gradually decreases with the RAMEB concentration, and these changes can be related to the formation of less well-defined objects with more flexible interfaces.

A remarkable increase in the growth rate of these supramolecular assemblies was noticed upon addition of larger amounts of RAMEB ranging from 100 to 130 mg/mL. Thus, for 100 mg/mL RAMEB, the apparent hydrodynamic radius is abruptly shifted to 31 nm, and this value far exceeds the dimension of the bare P123 micelles even when the PEO and PPO chains are in a fully extended conformation. This result suggests a possible modification of the interfacial curvature of the RAMEB-loaded micelles with transitions from spherical to ellipsoidal micelles. Similar behaviors have already been observed with the Pluronic P123 in the presence of different salts, which can further induce sphere-to-rod transitions of the micelles by dehydration of the hydrophilic corona.[55] The sphere-to-rod micellar shape transition is usually manifested by a simultaneous increase in the micellar growth rate and viscosity at room temperature.

For 130 mg/mL RAMEB, the band assigned to swollen micelles shrinks while a new population centered at ∼160 nm appears, indicating a transition toward a different type of large scattering species, which no longer resemble swollen micelles. Observations under a polarized light microscope of this sample revealed no sign of birefringence, suggesting that isotropic structures are the dominant species.

To obtain further information on the micellar growth, the viscosity of the copolymer solutions as a function of the RAMEB concentration was measured. Figure 5 shows the apparent viscosity vs shear rate plots recorded at 25 °C.

As can be seen, with the addition of increasing amounts of RAMEB, the micellar growth is accompanied by an enhancement of the viscosity and a modification of the rheological behavior of the micellar solutions. Therefore, the cyclodextrin-free P123 solution presents a near-Newtonian behavior since the apparent viscosity remains nearly constant (∼1.6 mPa·s) over the entire range of shear rates (0−130 s^{-1}). Upon the addition of 30 and 60 mg/mL RAMEB, the apparent viscosity increases slightly to ∼1.8 and ∼2.2 mPa·s, respectively, without any appreciable change in the plot profile. Further addition of RAMEB to 80 and 100 mg/mL induces a shear-thinning behavior (i.e., the viscosity decreases with increasing the shear rate), as well as a more pronounced increase in viscosity, up to ∼2.4 and ∼3.2 mPa·s, respectively, as measured at 130 s^{-1}. This behavior is consistent with the fact that the swollen micelles develop under ellipsoidal structures, probably due to the ability of RAMEB to modify the micelle curvature, confirming the previous statement from our DLS results. Even more evident changes can be noticed upon addition of 130 mg/mL RAMEB where the apparent viscosity increases up to 4.7 mPa·s. Additionally, a more pronounced shear-thinning behavior is developed, which is consistent with the formation of very large structures previously observed by DLS measurements.

dx.doi.org/10.1021/ma4008303 | *Macromolecules* 2013, 46, 5672−5683

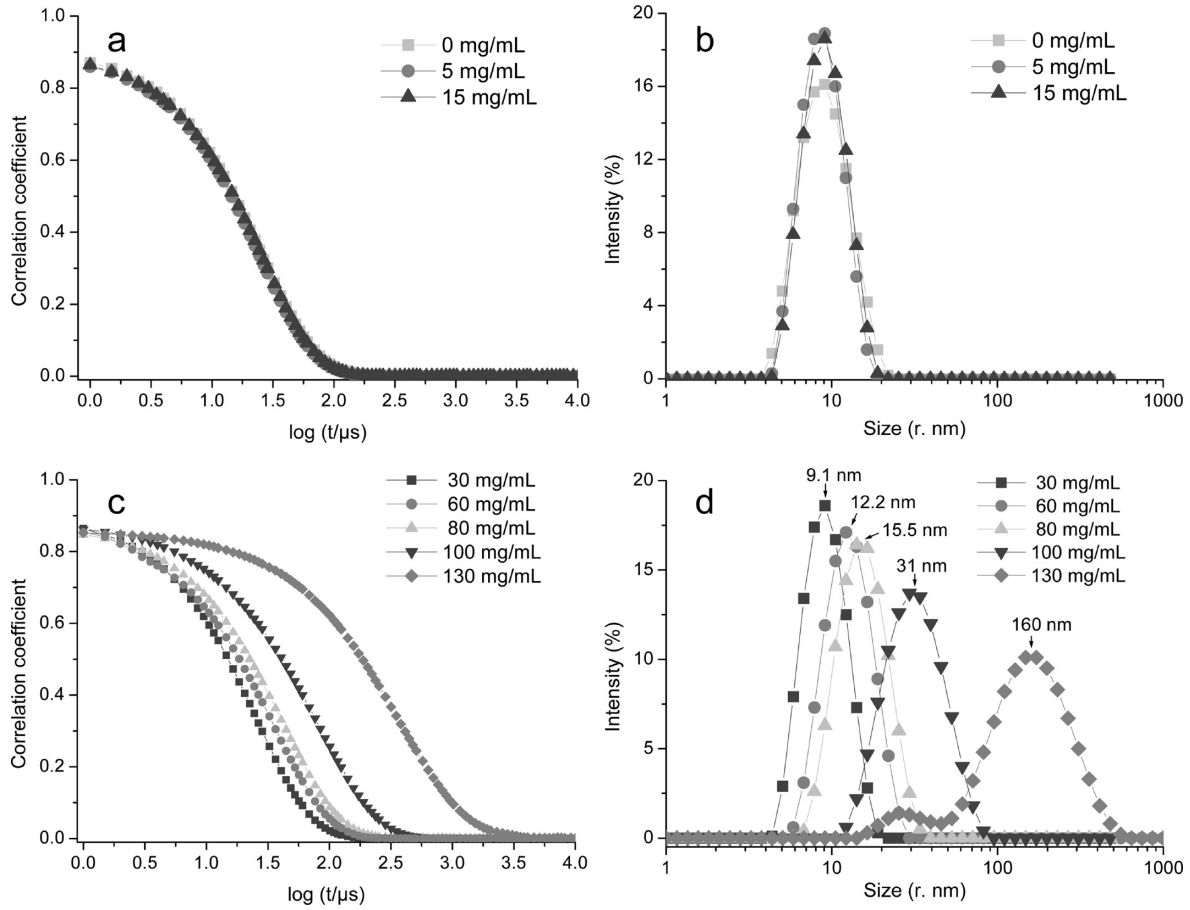

Figure 4. Correlation functions and corresponding apparent hydrodynamic radius (R_h) distributions of the scattered intensity for P123 solutions containing increasing amounts of RAMEB: 0, 5, 15 mg/mL (a, b) and 30, 60, 80, 100, 130 mg/mL (c, d) at 25 °C. For the sake of clarity, the investigated concentration domains are presented separately.

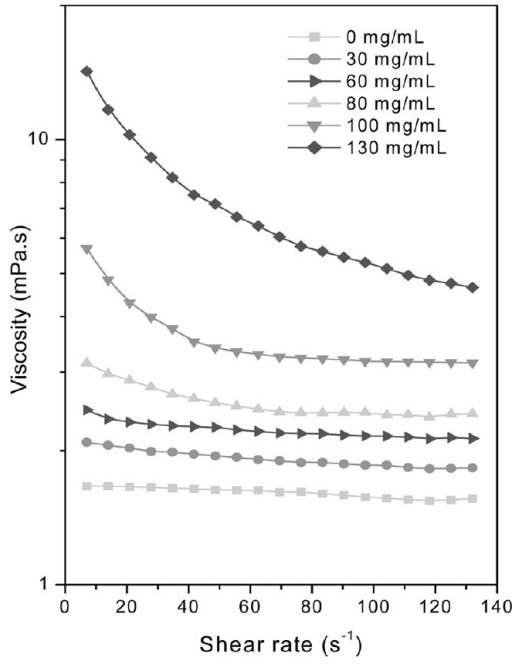

Figure 5. Apparent viscosity vs shear rate curves at 25 °C for micellar P123 solutions prepared with increasing amounts of RAMEB (0, 30, 60, 80, 100, and 130 mg/mL).

Synthesis of Mesoporous γ-Al_2O_3 from Cyclodextrin/Copolymer Templates. Motivated by the finding that the controlled addition of randomly methylated β-cyclodextrin to P123 solution promotes the micellar growth, especially in the range of 30−130 mg/mL, we have considered using these supramolecular coassemblies as potential templates in the synthesis of mesoporous alumina, with attempt to provide materials with tailored pore size and improved textural properties. With this aim, a series of mesoporous γ-Al_2O_3 were prepared by sol−gel synthesis with the nanoparticle procedure[34] using mixtures of P123 and RAMEB as micellar templates. The procedure is schematized in Figure 6. Briefly, in a first step, boehmite nanoparticles were synthesized in aqueous solution (H_2O/Al = 100) using aluminum tri-*sec*-butoxide ($Al(OBu)_3$) and nitric acid as the inorganic precursor and peptizing agent (HNO_3/Al = 0.07), respectively. In a second step, boehmite nanoparticles were allowed to self-assemble around the RAMEB/P123 assemblies at room temperature. Different molar ratios of RAMEB to P123 were employed, i.e., from 1.7 to 7.1 (concentration range of RAMEB of 30 to 130 mg/mL). After drying at 60 °C for 48 h, xerogels were calcined at 500 °C to remove the organic template and allow the transition from boehmite (AlO(OH)) to γ-Al_2O_3, which is assumed to occur at ∼380 °C as recently evidenced by thermal analysis.[41]

The efficiency of the template removal after the thermal treatment at 500 °C was evidenced by ATR-FTIR analysis. As

dx.doi.org/10.1021/ma4008303 | *Macromolecules* 2013, 46, 5672−5683

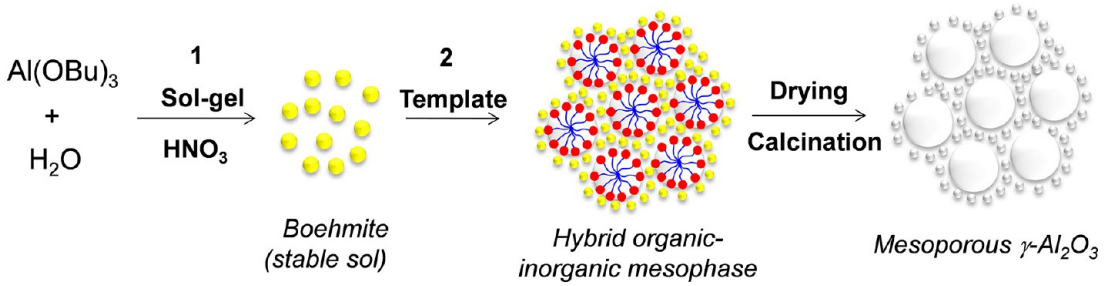

Figure 6. Schematic illustration of the two-step nanoparticle procedure (sol–gel and micelle template) used for the preparation of mesoporous alumina.

an illustrative example, Figure 7 shows the spectra recorded on the xerogels prepared with 80 mg/mL RAMEB (i.e., P1-CD80-Al sample) before and after calcination. In addition to the vibration modes of boehmite,[58,59] the spectrum of the hybrid xerogel presents strong intense bands at 965, 1010, 1035, and 1155 cm^{-1} which can be assigned to vibrational modes of the glycosyl units in the cyclodextrin molecules.[60,61] Another strong peak at 1085 cm^{-1} is assigned to the C–O–C stretching vibration of Pluronic P123. Moreover, the peak at 1367 cm^{-1} corresponds to free NO_3^- anions from HNO_3 added for the peptization.[62] The C–H vibrations bands from the P123 block copolymer and the cyclodextrin appear in the range of 2930–2850 cm^{-1}.

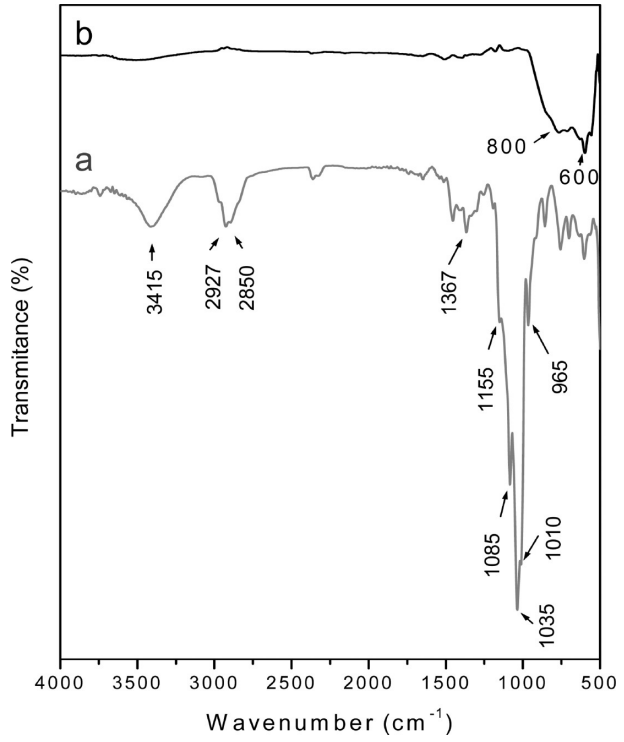

Figure 7. ATR-FTIR spectra of the P1-CD80-Al xerogel (PEO/Al = 1 and 80 mg/mL RAMEB) dried at 60 °C (a) and calcined at 500 °C (b).

As shown in the spectrum of the calcined sample, all those bands are almost eliminated while a wide unresolved pattern, extending from 510 to 950 cm^{-1} develops, which is typical of the distorted crystallographic structure of partially hydroxylated γ-Al_2O_3.[63,64] The two maxima at ~600 and ~800 cm^{-1} are characteristic of the stretching modes of AlO_6 and AlO_4 coordination groups, respectively. This confirms that the organic template has been efficiently removed from the pores of the mesoporous material after calcination at 500 °C while boehmite has been transformed in γ-Al_2O_3. This transformation was further evidenced by XRD measurements (Figure 8) with the presence of strong reflection lines characteristic of a well-crystallized γ-Al_2O_3 phase (JCPDS Card No. 10-0425).

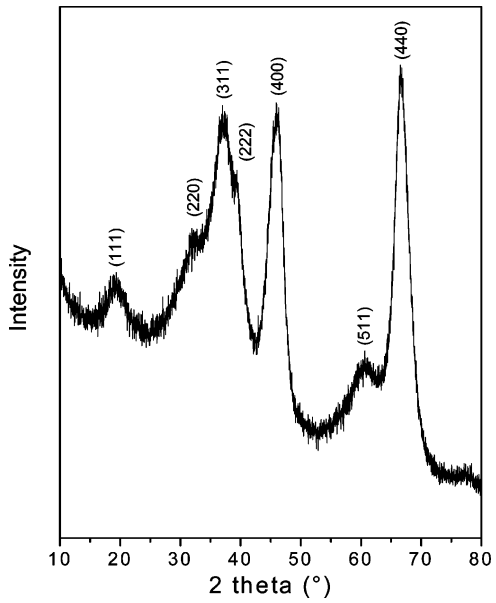

Figure 8. XRD pattern of the mesoporous γ-Al_2O_3 (PEO/Al = 1 and 80 mg/mL RAMEB) calcined at 500 °C.

To obtain further information about the textural properties of the calcined mesoporous alumina, nitrogen adsorption–desorption analyses were carried out and the results are given in Figure 9 and Table 1. It can be seen that all isotherms present a distinct H1 hysteresis loop characteristic of mesoporous materials.[65] The control sample, prepared without template, presents a capillary condensation step that starts at a relative pressure (P/P_0) of about 0.4, indicating the presence of small mesopores. The corresponding pore size distribution (PSD) plot is relatively narrow and centered at 5.6 nm and can be attributed to the assembly of several crystallites in rather compact rearrangements with "card-pack" microstructures.[41] Upon addition of the copolymer (P1-Al-T500 sample), a steep rise in the nitrogen uptake is observed at relative pressures P/P_0 > 0.8, indicating the formation of large mesopores with a high pore volume. Accordingly, the corresponding PSD plot indicates a dramatic increase in the pore size (from 5.6 to

dx.doi.org/10.1021/ma4008303 | Macromolecules 2013, 46, 5672–5683

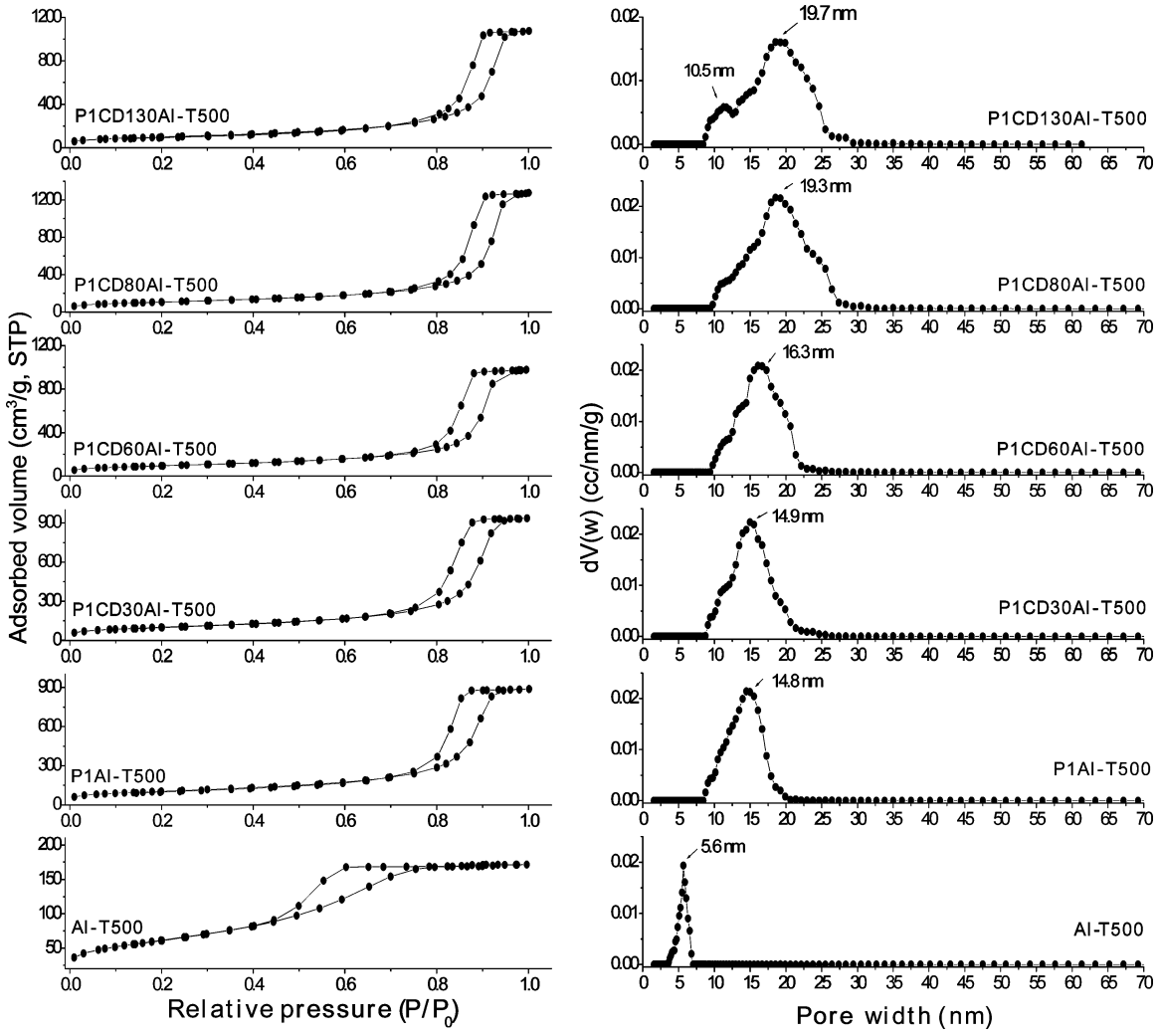

Figure 9. Evolution of adsorption−desorption isotherms (left-hand side) and corresponding pore size distributions (right-hand side) for the mesoporous γ-Al_2O_3 prepared without copolymer, with copolymer (PEO/Al = 1) and with increasing amounts of RAMEB (30−130 mg/mL).

Table 1. Textural Characteristics of Mesoporous γ-Al_2O_3 Calcined at 500 °C[a]

sample	S_{BET} (m^2 g^{-1})	PV (cm^3 g^{-1})	S_{cum} (m^2 g^{-1})	V_{cum} (cm^3 g^{-1})	PS (nm)
Al-T500	219	0.28	227	0.26	5.6
P1−Al-T500	357	1.37	387	1.35	14.8
P1-CD30-Al-T500	354	1.45	387	1.43	14.9
P1-CD60-Al-T500	356	1.62	372	1.60	16.3
P1-CD80-Al-T500	382	1.97	427	1.94	19.3
P1-CD130-Al-T500	360	1.66	373	1.63	10.5, 19.7

[a]P = [PEO]/[Al], CD = RAMEB concentration in the sol (mg/mL), T = calcination temperature, S_{BET} = BET specific surface area determined in the relative pressure range 0.1−0.25, PV = pore volume calculated from adsorbed volume at P/P_0 = 0.995, S_{cum}, V_{cum}, PS = cumulative surface area, cumulative volume, and pore size resulting from NLDFT calculations.

14.8 nm) and pore volume (from 0.28 to 1.37 cm^3/g) due to the formation of micelles acting as templates around which the self-assembly of nanoparticles occurs. Notably, the textural characteristics are still improved when RAMEB is added to the P123 copolymer micellar solution.

With increasing the cyclodextrin concentration in the range of 30−80 mg/mL, a progressive increase of the pore size is observed together with an enhancement of the pore volume (Table 1). The most striking textural properties are obtained for the sample prepared with 80 mg/mL having an average pore size of 19.3 nm, a pore volume of 1.97 cm^3/g, and a specific surface area of 382 m^2/g. Such an enhancement in the sample porosity upon addition of RAMEB can be directly attributed to its swelling effect on the copolymer assemblies, in line with the trend observed by DLS measurements.

However, when the cyclodextrin concentration is increased up to 130 mg/mL, the pore volume slightly shrinks to 1.66 cm^3/g, and a second mesopore population appears at about 10.5 nm, in addition to the one centered at 19.7 nm. Actually this second population of mesopores appears as a shoulder for the lowest cyclodextrin concentration (30 mg/mL), and it is transformed in a well-defined peak for 130 mg/mL RAMEB

dx.doi.org/10.1021/ma4008303 | Macromolecules 2013, 46, 5672−5683

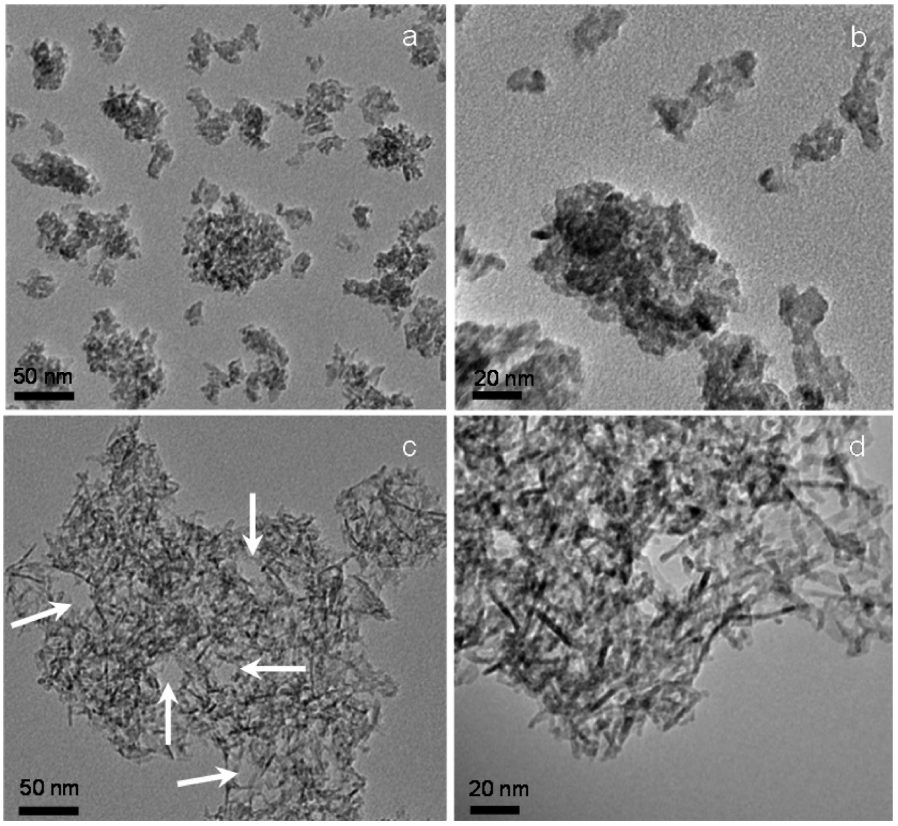

Figure 10. TEM images taken at two different magnifications for mesoporous γ-Al_2O_3 synthesized without template (a, b) and with a mixture of P123 (PEO/Al = 1) and RAMEB (80 mg/mL) (c, d). Samples were calcined at 500 °C.

due to the formation of more aggregates acting as template. We do not exclude the possibility that during the coassembly process the constraint exerted by the solid boehmite nanoparticles on the swollen micelles provokes a release of a part of the cyclodextrin from the PEO−PPO interfaces, therefore generating a second porosity which becomes more clearly defined as the micelles are more loaded in RAMEB.

Note that an additional control sample (not shown) prepared with 130 mg/mL RAMEB but without copolymer, indicated that much smaller pores (8.1 nm) are produced. This result is indicative of the fact that the largest mesopores formed at 19.7 nm are attributed to the swollen micelles, whereas the smallest mesopores observed at 10.5 nm account for possible small complexes formed by the association of block copolymer unimers and excess cyclodextrin that has not interacted with copolymer. Finally, our results from N_2 adsorption analyses have shown that, with a controlled addition of RAMEB to the copolymer micellar solution, mesoporous alumina with tunable pore size and pore volume can be easily prepared. It is interesting to note that such remarkable textural characteristics are obtained in aqueous solution (H_2O/Al = 100) by a room temperature self-assembly synthesis procedure, without any need of hydrothermal treatment.

From the representative TEM images of the mesoporous γ-Al_2O_3 prepared without and with template (PEO/Al = 1 and 80 mg/mL RAMEB) (Figure 10), the effect of the supramolecular assemblies on the network structure can be clearly visualized. Therefore, it can be seen that the mesoporous γ-Al_2O_3 prepared without template is comprised of aggregated particles with no regular shape and a low interparticle porosity. By contrast, the P1-CD80-Al-T500 material shows a well-defined fiberlike morphology indicating the important role of the template in restructuring the particle network. Interestingly, in addition to the fiberlike morphology, several voids with an average diameter of ∼20 nm, similar to the pore size determined from N_2 adsorption measurements, are also present at a very high yield throughout the nanoparticle network (see arrows in Figure 10c). This result is a strong indication of the fact that, after the thermal treatment, the material has successfully adopted some characteristics of the supramolecular template. Hence, the void space formed between the nanoparticle assemblies may be seen as a solid negative replica of the original swollen micelles formed by the coassembly of copolymer and cyclodextrin.

■ DISCUSSION

Taken together, our data provide evidence that the supramolecular structures with controlled compositions of Pluronic P123 block copolymer and RAMEB can be successfully used as soft templates to produce pure mesoporous γ-Al_2O_3 materials after the removal of the template. Interestingly, the structural changes occurring in solution, within the polymer micelles, can be applied to design mesoporous alumina with smoothly varying pore sizes and morphologies.

In our investigation of the P123−RAMEB mixed system, both surface tension and DLS measurements clearly show that while cyclodextrin aggregates abruptly disrupt to interact preferentially with Pluronic micelles, these latter remain intact upon addition of the cyclodextrin. Although no micellar disruption occurs, the question that arises is whether RAMEB locates preferentially in the hydrophilic shell of the copolymer micelles or rather solubilizes in the hydrophobic core through

dx.doi.org/10.1021/ma4008303 | *Macromolecules* 2013, 46, 5672−5683

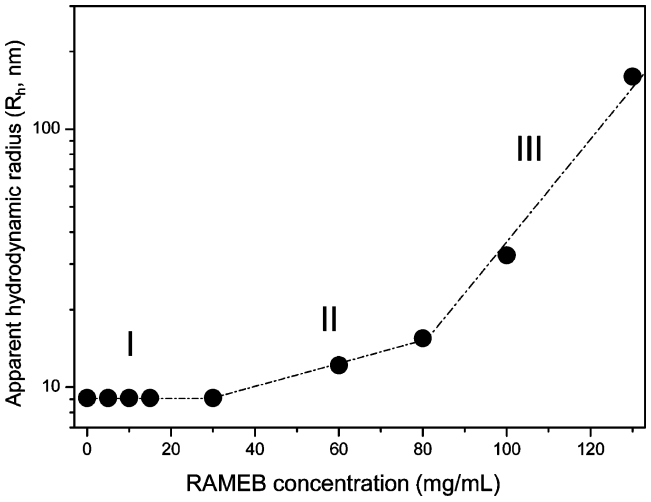

Figure 11. Evolution of the apparent hydrodynamic radius, R_h as a function of RAMEB concentration for the cyclodextrin/copolymer supramolecular assemblies formed at 25 °C.

interactions with the PPO blocks. This is an important feature since it is well-known that the location of a solubilizate molecule within the micelles plays an important role in determining the extent of the micellar growth.[66,67] The micellar shape transition in Pluronic systems depends on several parameters and in particular on the chemical nature of the additive. In the case of RAMEB, the random substitution of hydroxyl groups by a relatively large number of hydrophobic methoxy groups (~12.6) strongly affects the chemical properties of β-cyclodextrins, with dramatic changes both in the solubility profile (compared to β-CD by the disruption of intermolecular hydrogen bonds)[11] and in the interfacial behavior. Indeed, it has already been shown by surface tension measurements carried out on RAMEB that the partial methylation of β-CD greatly improved its surface active properties due to the presence of more hydrophobic microenvironments.[39] Therefore, it can be assumed that RAMEB has marked hydrophobic and hydrophilic domains, which can interact in a specific way with the PEO and PPO blocks of Pluronic P123. Our experimental results indicate that, depending on the amount of added cyclodextrin, these interactions may affect both the size and shape of the micelles. On the basis of the DLS results, the semilog plot of the apparent hydrodynamic radius vs RAMEB concentration shows that the extent of the micellar growth is characterized by the existence of three concentration regimes, as evidenced in Figure 11.

For low RAMEB concentrations, in the range of 5−30 mg/mL (region I), it can be seen that no significant change in the apparent size of the micelles occurs, suggesting that the cyclodextrin first interacts with the hydrated PEO groups in the micellar corona by hydrogen bonding through its OH groups.

With further cyclodextrin addition, in the range of 30−80 mg/mL (region II), a progressive increase in the apparent hydrodynamic radius from 9.1 to 15.5 nm is evidenced. This may be explained by the association of this cyclodextrin with block copolymer molecules giving rise to swollen micelles, which progressively grow in size as more and more RAMEB is added. In addition, viscosity measurements provided evidence of the existence of a shear-thinning effect, in which supramolecular assemblies tend to form elongated shapes. Such a behavior is typical of block copolymers. Indeed, a shape transition from spherical to rod-like or prolate ellipsoidal structures has been observed with a number of Pluronic micelles under different solution conditions, such as in the vicinity of the cloud point[68] as well as in the presence of salts (NaCl, KCl, KF)[55,69] or nonionic surfactants.[70] Under such conditions, the micelles undergo a restructuring process, which is manifested by an expansion of their size and a concomitant increase in the viscosity of the copolymer solution due to the entanglement of elongated micelles.[55,68,70] Similarly from the ternary P123/water/butanol phase diagram, a transition from spherical micelles to lamella has also been evidenced in the presence of butanol, and this change has been connected to the affinity of the alcohol for the interfacial region of the Pluronic micelles reducing their interfacial curvature.[29] On the basis of these studies, our results suggest that, in this intermediate concentration regime, the binding of RAMEB can be considered as a solubilization within the block copolymer micelles. Indeed, considering the surface-active properties of RAMEB and its dual hydrophilic−hydrophobic nature, this cyclodextrin probably behaves like a cosurfactant having a preferential affinity for the PEO−PPO interface layer of the micelles. The preferred location of RAMEB in this interfacial area contributes to the swelling of the micelles and to the decrease of the micellar curvature from spherical to ellipsoidal shape. A scheme proposed for the copolymer micellar growth upon addition of RAMEB in this concentration region is shown in Figure 12 where the progression of the supramolecular structures from spherical micelles to swollen ellipsoidal micelles with increasing RAMEB concentration reflects the change in the interfacial curvature modulated by the cyclodextrin.

For still higher RAMEB concentrations, in the range of 100−130 mg/mL (region III), large scattering species with an apparent hydrodynamic radius as high as 160 nm are detected.

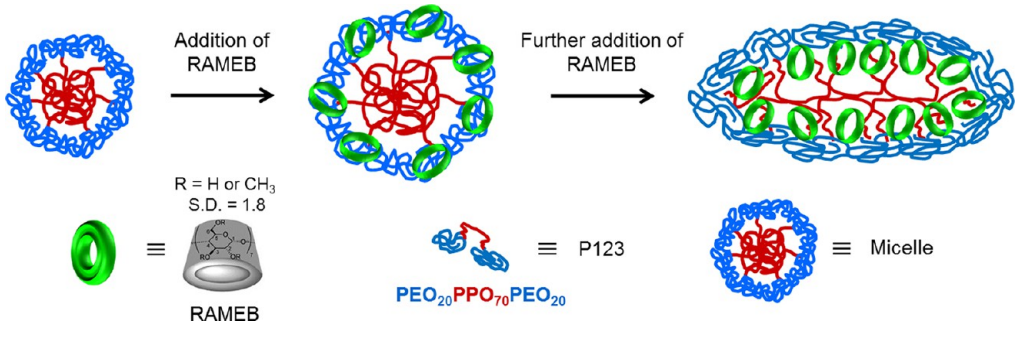

Figure 12. Schematic representation of the solubilization of RAMEB within the P123 copolymer micelles in the region II (30−80 mg/mL RAMEB).

dx.doi.org/10.1021/ma4008303 | Macromolecules 2013, 46, 5672−5683

In a second set of experiment, we have taken advantage of this fundamental knowledge in the supramolecular assemblies, formed by randomly methylated β-CD and Pluronic P123 block copolymer, to prepare mesoporous alumina with adjustable pore size. The results obtained from both N_2 adsorption measurements and TEM observations confirm that RAMEB acts as an efficient swelling agent for the pore expansion and pore volume enhancement of γ-Al_2O_3. Therefore, when the previously investigated RAMEB-swollen micelles were used as templates (region II), mesoporous alumina with adjustable pore size, from 14.9 to 19.3 nm, was obtained. The modulation of the pore size and structure gives strong indication that the supramolecular assemblies have been replicated by the nanoparticle assembly process. Additionally, a pore volume as high as ~2 cm^3/g was obtained with 80 mg/mL RAMEB, which to the best of our knowledge has not been reported so far with other templates under mild conditions. Such porous material may be of high interest for applications dedicated to heterogeneous catalysis[71−73] or sorption processes (e.g., heavy metals,[74] CO_2 capture[75]), for which supports with high adsorption capacity are required.

CONCLUSIONS

In conclusion, we have developed a new template directed strategy for the synthesis of mesoporous γ-Al_2O_3 materials with tunable pore size by taking advantage of the ability of the randomly methylated β-cyclodextrin (RAMEB) to act as a micelle expander. By locating at the PEO−PPO interface of the Pluronic micelles, RAMEB allows to increase the size of the templating assemblies at a higher extent than the so far reported hydrocarbons, offering new insights in the modern material science for the generation of well-defined template structures with enlarged pores. This finding would be of interest in the fields of adsorption and heterogeneous catalysis for environmental and sustainable energy applications (e.g., Fischer−Tropsch process for the production of synthetic fuels).

AUTHOR INFORMATION

Corresponding Author

*E-mail: anne.ponchel@univ-artois.fr.

Notes

The authors declare no competing financial interest.

ACKNOWLEDGMENTS

The TEM facility in Lille (France) is supported by the Conseil Regional du Nord-Pas de Calais and the European Regional Development Fund (ERDF). The authors are also grateful to Laurence Burylo (UCCS, University of Lille, France) for the XRD measurements.

REFERENCES

(1) Wenz, G. *Angew. Chem., Int. Ed. Engl.* **1994**, *33*, 803−822.
(2) Born, M.; Ritter, H. *Angew. Chem., Int. Ed. Engl.* **1995**, *34*, 309−311.
(3) Jeromin, J.; Ritter, H. *Macromolecules* **1999**, *32*, 5236−5239.
(4) Harada, A. *Acc. Chem. Res.* **2001**, *34*, 456−464.
(5) Harada, A. *Coord. Chem. Rev.* **1996**, *148*, 115−133.
(6) Herrmann, W.; Keller, B.; Wenz, G. *Macromolecules* **1997**, *30*, 4966−4972.
(7) Li, G.; McGown, L. B. *Science* **1994**, *264*, 249−251.
(8) Cacialli, F.; Wilson, J. S.; Michels, J. J.; Daniel, C.; Silva, C.; Friend, R. H.; Severin, N.; Samori, P.; Rabe, J. P.; O'Connell, M. J.; Taylor, P. N.; Anderson, H. L. *Nat. Mater.* **2002**, *1*, 160−164.
(9) Medintz, I. L.; Clapp, A. R.; Mattoussi, H.; Goldman, E. R.; Fisher, B.; Mauro, J. M. *Nat. Mater.* **2003**, *2*, 630−638.
(10) Alexandridis, P. *Curr. Opin. Colloid Interface Sci.* **1997**, *2*, 478−489.
(11) Szejtli, J. *Chem. Rev.* **1998**, *98*, 1743−1753.
(12) Breslow, R.; Dong, S. D. *Chem. Rev.* **1998**, *98*, 1997−2011.
(13) Harada, A.; Kamachi, M. *Macromolecules* **1990**, *23*, 2821−2823.
(14) Harada, A.; Li, J.; Kamachi, M. *Macromolecules* **1993**, *28*, 5698−5703.
(15) Harada, A.; Hashidzume, A.; Yamaguchi, H.; Takashima, Y. *Chem. Rev.* **2009**, *109*, 5974−6023 and references therein.
(16) Fujita, H.; Ooya, T.; Kurisawa, M.; Mori, H.; Terano, M.; Yui, N. *Macromol. Rapid Commun.* **1996**, *17*, 509−515.
(17) Fujita, H.; Ooya, T.; Yui, N. *Macromolecules* **1999**, *32*, 2534−2541.
(18) Tsai, C. C.; Leng, S.; Jeong, K. U.; Van Horn, R. M.; Wang, C. L.; Zhang, W. B.; Graham, M. J.; Huang, J.; Ho, R. M.; Chen, Y.; Lotz, B.; Cheng, S. Z. D. *Macromolecules* **2010**, *43*, 9454−9461.
(19) Perry, C.; Hebraud, P.; Gernigon, V.; Brochon, C.; Lapp, A.; Lindner, P.; Schlatter, G. *Soft Matter* **2011**, *7*, 3502−3512.
(20) Wang, J.; Jiang, M. *J. Am. Chem. Soc.* **2006**, *128*, 3703−3708.
(21) Giacomelli, C.; Schmidt, V.; Putaux, J. L.; Narumi, A.; Kakuchi, T.; Borsali, R. *Biomacromolecules* **2009**, *10*, 449−453.
(22) Gaitano, G. G.; Brown, W.; Tardajos, G. *J. Phys. Chem. B* **1997**, *101*, 710−719.
(23) Joseph, J.; Dreiss, C. A.; Cosgrove, T.; Pedersen, J. S. *Langmuir* **2007**, *23*, 460−466.
(24) Lazzara, G.; Milioto, S. *J. Phys. Chem. B* **2008**, *112*, 11887−11895.
(25) Nogueiras-Nieto, L.; Alvarez-Lorenzo, C.; Sandez-Macho, I.; Concheiro, A.; Otero-Espinar, F. J. *J. Phys. Chem. B* **2009**, *113*, 2773−2782.
(26) Dreiss, C. A.; Nwabunwann, E.; Liu, R.; Brooks, N. *Soft Matter* **2009**, *5*, 1888−1896.
(27) Tsai, C. C.; Zhang, W.-B.; Wang, C.-L.; Van Horn, R. M.; Graham, M. J.; Huang, J.; Chen, Y.; Guo, M.; Cheng, S. Z. D. *J. Chem. Phys.* **2010**, *132*, 204903.
(28) Valero, M.; Grillo, I.; Dreiss, C. A. *J. Phys. Chem. B* **2012**, *116*, 1273−1281.
(29) Holmqvist, P.; Alexandridis, P.; Lindman, B. *J. Phys. Chem B* **1998**, *102*, 1149−1158.
(30) Polarz, S.; Smarsly, B.; Bronstein, L.; Antonietti, M. *Angew. Chem., Int. Ed.* **2001**, *40*, 4417−4421.
(31) Han, B. H.; Antonietti, M. *Chem. Mater.* **2002**, *14*, 3477−3485.
(32) Han, B. H.; Smarsly, B.; Gruber, C.; Wenz, G. *Microporous Mesoporous Mater.* **2003**, *66*, 127−132.
(33) Kruk, M. *Acc. Chem. Res.* **2012**, *45*, 1678−1687.
(34) Bleta, R.; Alphonse, P.; Lorenzato, L. *J. Phys. Chem C* **2010**, *114*, 2039−2048.
(35) Su, B. L.; Sanchez, C.; Yang, X. Y. In *Hierarchically Structured Porous Materials. From Nanoscience to Catalysis, Separation, Optics, Energy, and Life Science*; Su, B. L., Sanchez, C., Yang, X. Y., Eds.; Wiley-VCH: Weinheim, 2012.
(36) Huang, L.; Yan, X.; Kruk, M. *Langmuir* **2010**, *26*, 14871−14878.
(37) Fan, J.; Yu, C.; Lei, J.; Zhang, Q.; Li, T.; Tu, B.; Zhou, W.; Zhao, D. *J. Am. Chem. Soc.* **2005**, *127*, 10794−10795.
(38) Uekama, K.; Irie, T. In *Cyclodextrins and Their Industrial Uses*; Duchêne, D., Ed.; Editions de la Santé: Paris, 1987; pp 395−439.
(39) Leclercq, L.; Bricout, H.; Thilloy, S.; Monflier, E. *J. Colloid Interface Sci.* **2007**, *307*, 481−487.
(40) Ferreira, M.; Bricout, H.; Azaroual, N.; Landy, D.; Tilloy, S.; Hapiot, F.; Monflier, E. *Adv. Synth. Catal.* **2012**, *354*, 1337−1346.
(41) Bleta, R.; Alphonse, P.; Pin, L.; Gressier, M.; Menu, M. J. *J. Colloid Interface Sci.* **2012**, *367*, 120−128.
(42) Niesz, K.; Yang, P.; Somorjai, G. A. *Chem. Commun.* **2005**, 1986−1987.
(43) Misra, C. In *Industrial Alumina Chemicals*; ACS Monograph 184; American Chemical Society: Washington, DC, 1986.

(44) Radhakrishnan, R.; Oyama, S. T.; Chen, J. G.; Asakura, K. *J. Phys. Chem. B* **2001**, *105*, 4245−4253.
(45) Schüth, F.; Unger, K. In *Preparation of Solid Catalysts*; Ertl, G., Knözinger, H., Weitkamp, J., Eds.; Wiley-VCH: Weinheim, 1999; pp 77−80.
(46) Yoldas, B. E. *Am. Ceram. Soc. Bull.* **1975**, *54*, 289−290.
(47) Alphonse, P.; Courty, M. *J. Colloid Interface Sci.* **2005**, *290*, 208−219.
(48) Berne, B. J.; Pecora, R. In *Dynamic Light Scattering with Applications to Chemistry, Biology and Physics*, 2nd ed.; Dover Publications: New York, 2000.
(49) Provencher, S. W. *Comput. Phys. Commun.* **1982**, *27*, 213−227.
(50) Evans, R.; Marconi, U. M. B.; Tarazona, P. *J. Chem. Soc., Faraday Trans. 2* **1986**, *82*, 1763−1787.
(51) Alexandridis, P.; Holzwarth, J. F.; Hatton, T. A. *Macromolecules* **1994**, *27*, 2414−2425.
(52) Alexandridis, P.; Holzwarth, J. F.; Hatton, T. A. *J. Am. Oil Chem. Soc.* **1995**, *72*, 823−830.
(53) Bernat, V.; Ringard-Lefebvre, C.; Bas, G. L.; Perly, B.; Djedaïni-Pilard, F.; Lesieur, S. *Langmuir* **2008**, *24*, 3140−3149.
(54) Mahata, A.; Bose, D.; Ghosh, D.; Jana, B.; Bhattacharya, B.; Sarkar, D.; Chattopadhyay, N. *J. Colloid Interface Sci.* **2010**, *347*, 252−259.
(55) Kadam, Y.; Ganguly, R.; Kumbhakar, M.; Aswal, V. K.; Hassan, P. A.; Bahadur, P. *J. Phys. Chem. B* **2009**, *113*, 16296−16302.
(56) Gonzalez-Gaitano, G.; Rodriguez, P.; Isasi, J. R.; Fuentes, M.; Tardajos, G.; Sanchez, M. *J. Incl. Phenom. Macrocycl. Chem.* **2002**, *44*, 101−105.
(57) Herbois, R.; Noel, S.; Léger, B.; Bai, L.; Roucoux, A.; Monflier, E.; Ponchel, A. *Chem. Commun.* **2012**, *48*, 3451−3453.
(58) Fripiat, J. J.; Bosmans, H.; Bouxhet, P. G. *J. Phys. Chem.* **1967**, *71*, 1097−1111.
(59) Colomban, Ph. *J. Mater. Sci.* **1989**, *24*, 3002−3010.
(60) Egyed, O. *Spectroscopy* **1990**, *1*, 225−227.
(61) Ponchel, A.; Abramson, S.; Quartararo, J.; Bormann, D.; Barbaux, Y.; Monflier, E. *Microporous Mesoporous Mater.* **2004**, *75*, 261−272.
(62) Bleta, R.; Jaubert, O.; Gressier, M.; Menu, M. J. *J. Colloid Interface Sci.* **2011**, *363*, 557−565.
(63) Rinaldi, R.; Schuchardt, U. *J. Catal.* **2005**, *236*, 335−345.
(64) Priya, G. K.; Padmaja, P.; Warrier, K. G. K.; Damodaran, A. D.; Aruldhas, G. *J. Mater. Sci. Lett.* **1997**, *16*, 1584−1587.
(65) Sing, K. S. W.; Everett, D. H.; Haul, R. A. W.; Moscou, L.; Pierotti, R. A.; Rouquerol, J.; Siemieniewska, T. *Pure Appl. Chem.* **1985**, *57*, 603−619.
(66) Hoffmann, H.; Ulbricht, W. *J. Colloid Interface Sci.* **1989**, *129*, 388−405.
(67) Bayer, O.; Hoffmann, H.; Ulbricht, W.; Thurn, H. *Adv. Colloid Interface Sci.* **1986**, *26*, 177−203.
(68) Ganguly, R.; Choudhury, N.; Aswal, V. K.; Hassan, P. A. *J. Phys. Chem. B* **2009**, *113*, 668−675.
(69) Denkova, A. G.; Mendes, E.; Coppens, M. O. *J. Phys. Chem. B* **2008**, *112*, 793−801.
(70) Lof, D.; Schillén, K.; Torres, M. F.; Müller, A. J. *Langmuir* **2007**, *23*, 11000−11006.
(71) Morterra, C.; Magnacca, G. *Catal. Today* **1996**, *27*, 497−532.
(72) Jean-Marie, A.; Griboval-Constant, A.; Khodakov, A. Y.; Monflier, E.; Diehl, F. *Chem. Commun.* **2011**, *47*, 10767−10769.
(73) Einaga, H.; Futamura, S. *J. Catal.* **2004**, *227*, 304−312.
(74) Cai, W. Q.; Yu, J. G.; Jaroniec, M. *J. Mater. Chem.* **2010**, *20*, 4587−4594.
(75) Chen, C.; Ahn, W.-S. *Chem. Eng. J.* **2011**, *166*, 646−651.

■ NOTE ADDED AFTER ASAP PUBLICATION

This article posted ASAP on July 5, 2013. Figures 6 and 12 have been revised. The correct version posted on July 10, 2013.